

## Exact Calculation of the Reflection Coefficient for Coated Optical Waveguide Devices

By D. R. KAPLAN\* and P. P. DEIMEL\*

(Manuscript received March 8, 1984)

We derive an exact solution to the problem of the reflection coefficient for a coated slab waveguide. A series of computer calculations apply these results to a  $\lambda = 1.3 \mu\text{m}$  InGaAsP laser with an active area of 0.2 micron, an active area index of refraction of 3.51, and a cladding index of refraction of 3.22. Our results show that the correction due to the index step is a few percent for an uncoated laser. For antireflection coatings (reflectivity less than 1 percent), the correction due to the index step is significant. These results are important in choosing coating indices and thicknesses when minimum reflectivities are desired (e.g., for a superluminescent diode). The results, calculated over a range of indices of refraction of the coating, show that the TE and TM reflectivities are minimized at about the same value of the index, 1.84. However, the coating thicknesses at which the reflectivity is minimized are different for the TE and TM case. For example, when the TE reflectivity is minimized, the TM reflectivity exceeds the TE reflectivity by over two orders of magnitude.

### I. INTRODUCTION

The reflectivity of light from optical waveguide devices can be modified by the application of suitably chosen coatings. Examples of waveguide devices include semiconductor lasers, optical switches, optical modulators, and optical fibers. In this paper an exact solution to the problem of the reflectivity from single transverse mode, two-dimensional waveguide devices (such as slab waveguides) is derived

---

\* AT&T Bell Laboratories.

---

Copyright © 1984 AT&T. Photo reproduction for noncommercial use is permitted without payment of royalty provided that each reproduction is done without alteration and that the Journal reference and copyright notice are included on the first page. The title and abstract, but no other portions, of this paper may be copied or distributed royalty free by computer-based and other information-service systems without further permission. Permission to reproduce or republish any other portion of this paper must be obtained from the Editor.

and the results are applied to a typical gain-guided semiconductor laser. The calculation is only limited to a single transverse mode for convenience. The extension to a multimode system is straightforward.

The problem of reflectivity from an uncoated laser was described in detail by McKenna<sup>1</sup> and his method was employed by Reinhart et al.,<sup>2</sup> Gordon,<sup>3</sup> and Krupka.<sup>4</sup> The eigenstates in the waveguide consist of a discrete set of bound modes and a continuous set of unbound modes. A numerical calculation for the uncoated laser was performed by Ikegami,<sup>5</sup> although he neglected the continuous part of the spectrum. Pudensi and Ferreira<sup>6</sup> have developed a method to correct for this by combining the continuous modes to form a discrete description of the continuum. Kardontchik<sup>7</sup> used a method similar to Ikegami to calculate the reflectivity for three-dimensional laser structures.

Clarke<sup>8</sup> suggested an approximate method to calculate the reflectivity from an antireflection coated laser. However, that approximation is based on truncating the angular spectrum of the incident bound state. This approximation is especially poor when the reflectivity is calculated for a coating close to the quarter-wave condition. The problem of mode conversion by reflection from the mirror facets in an uncoated laser was considered in detail by Lewin.<sup>9</sup>

## II. MODEL

The detailed derivation of the reflection coefficient is described in the Appendix. This section describes the model for the calculation and gives the analytical results.

The model used for this calculation is shown in Fig. 1. The wave incident on the boundary between regions 1 and 2 is described by a single bound state,  $\psi$ . The collection of all unbound states,  $\phi_k$ , plus the bound state,  $\psi$ , forms a complete orthogonal set inside the waveguide (region 1). The arrows labeling the states in Fig. 1 denote whether the state has a wave vector with a positive  $z$  component (e.g.,  $\vec{j}$ ) or negative  $z$  component (e.g.,  $\vec{j}$ ).

Inside the coating (region 2) the states may be described as an infinite sum of plane waves and evanescent fields. Finally, in air (region 3) the complete set is again a set of plane waves and evanescent fields.

The boundary between regions 1 and 2 cannot, in general, be described as the boundary between two uniform media. In addition, the states,  $\phi_k$ , are not plane waves. As a result, the Fresnel reflection coefficients,<sup>10</sup> which were used extensively in previous calculations,<sup>1-4,8</sup> are not, in principle, valid for this problem. We define  $\Delta n(x)$  as the difference between the refractive index inside the laser at position  $x$ , ( $n_1(x)$ ), and the refractive index of the cladding layers at position  $x =$

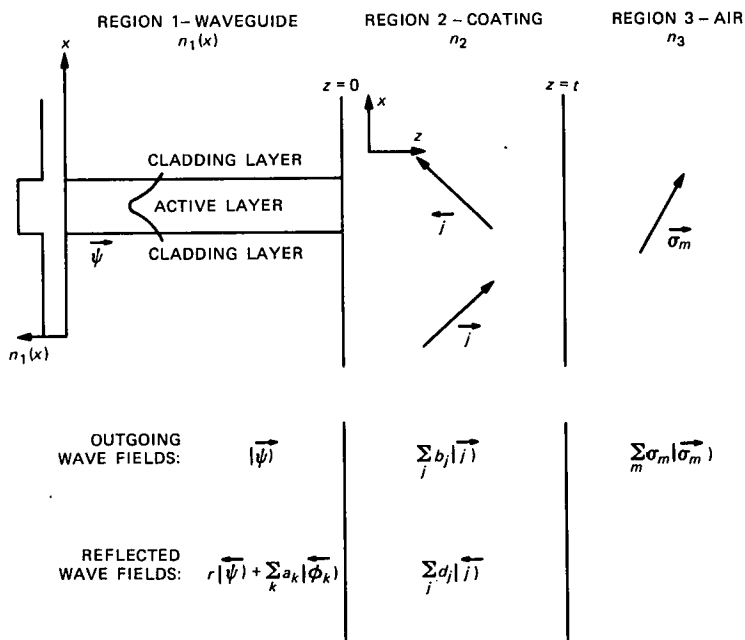


Fig. 1—Two-dimensional model used in calculation.

$\pm\infty$ , ( $n_1^0$ ). For the case of an asymmetric waveguide  $\Delta n(x)$  is the difference between the refractive index at position  $x$  and the average of the refractive index of the cladding layers at positions  $x = +\infty$  and  $x = -\infty$  (see Section III). In the limit that  $\Delta n(x)$  approaches zero for all  $x$ , the unbound states in region 1 again become plane waves and the Fresnel reflection coefficients are again valid. In this condition the bound state,  $\psi$ , can be expressed as a sum over plane waves.\* For each plane wave there is a different reflectivity at the interface between regions 1 and 2,  $r_{12}^j$ , where  $j$  denotes a particular plane wave transmitted into region 2.

The method adopted in this paper is to calculate the reflection coefficient,  $r$ , in the limit that  $\Delta n(x)$  approaches zero and then calculate an infinite perturbation expansion in terms of a suitably chosen integral of  $\Delta n(x)$ . By  $r$  we mean the amplitude for the bound state to reflect back onto the same bound state. This number is important in determining the threshold condition for semiconductor laser operation.

Since we are concerning ourselves with a slab waveguide, we can break the problem into the solution of TE modes and TM modes.

\* When  $\Delta n(x) = 0$  for all  $x$ , there are no bound states. In general,  $\psi$  corresponds to a sum of plane waves only at a given surface  $z = \text{constant}$ .

The results for the TE modes are

$$r_{\text{TE}} = \int_{-\infty}^{\infty} ds_2 f(s_2) f^*(s_2) R(s_2) + \int_{-\infty}^{\infty} ds_2 f^*(s_2) \Delta(s_2) \frac{[R(s_2) + 1]}{2n_1^0 h_1^0(s_2)}, \quad (1)$$

where the zeroth approximation to  $\Delta(s_2)$  is given by

$$\Delta^{(0)}(s_2) = \int_{-\infty}^{\infty} ds_2' \Delta H(s_2, s_2') f(s_2') (1 - R(s_2')), \quad (2)$$

and the  $i$ th approximation to  $\Delta(s_2)$  is

$$\Delta^{(i)}(s_2) = \Delta^{(0)}(s_2) - \int_{-\infty}^{\infty} ds_2' \Delta H(s_2, s_2') \Delta^{(i-1)}(s_2') \left[ \frac{R(s_2') + 1}{2n_1^0 h_1^0(s_2')} \right]. \quad (3)$$

The terms of the above expression are now described. The Fourier transform of the bound state,  $f(s_2)$ , is given by

$$f(s_2) = \frac{1}{\sqrt{\lambda_2}} \int_{-\infty}^{\infty} dx \bar{\psi}(x) e^{-ik_2 s_2 x}, \quad (4)$$

where  $\lambda_2$  is the wavelength of the light inside the coating,  $\lambda_0$  is the wavelength in vacuum,  $n_2$  is the index of the coating layer, and  $k_2 = 2\pi n_2 / \lambda_0$ . The complex conjugate of  $f(s_2)$  is given by  $f^*(s_2)$ . For  $|s_2| < 1$  in eqs. (1) through (4),  $s_2$  is equivalent to the  $\sin(\Theta)$ , where  $\Theta$  is the angle of the transmitted plane wave in the coating relative to the normal vector of the surface between regions 1 and 2. Also,  $R(s_2)$  is the Fresnel reflection coefficient for a field incident (at a coating angle  $\Theta$ ) onto the coated interface.<sup>10</sup> Thus,

$$R(s_2) = \frac{r_{12}(s_2) + r_{23}(s_2) e^{2i\phi(s_2)}}{1 + r_{12}(s_2)r_{23}(s_2) e^{2i\phi(s_2)}}, \quad (5)$$

where  $r_{12}$  is the Fresnel reflection coefficient for the semi-infinite boundary between regions 1 and 2,  $r_{23}$  is the Fresnel reflection coefficient between regions 2 and 3, and

$$\phi(s_2) = \frac{2\pi n_2 t}{\lambda_0} \sqrt{1 - s_2^2}. \quad (6)$$

The index of refraction of the coating is  $n_2$ . The thickness of the coating is  $t$ , and  $\lambda_0$  is the wavelength in vacuum.

Furthermore,

$$h_1^0(s_2) = \sqrt{1 - \left( \frac{n_2 s_2}{n_1^0} \right)^2}, \quad (7)$$

$$h_1(s_2, x) = \sqrt{1 - \left( \frac{n_2 s_2}{n(x)} \right)^2}, \quad (8)$$

and

$$\Delta H(s_2, s'_2) = \frac{n_2}{\lambda_0} e^{ik_0 n_2 x(s_2 - s'_2)} [h_1(s'_2, x)n_1(x) - h_1^0(s'_2)n_1^0], \quad (9)$$

where  $k_0 = 2\pi/\lambda_0$ .

The first term in eq. (1) is the Fresnel approximation to the reflection coefficient. The second term in eq. (1) is the correction due to the presence of  $\Delta n(x)$  in region 1. With eq. (3) the higher-order correction terms are calculable. These terms are negligible for the laser configuration described below.

Equation (5) shows how the reflection coefficient can easily be generalized for a multiple coating condition. The reflection coefficients,  $r_{12}(s_2)$  and  $r_{23}(s_2)$ , are single-interface Fresnel reflection coefficients. Only the interface between regions 2 and 3 plays a role in the coefficient  $r_{23}$ . For a multiple layer condition  $r_{23}$  is replaced by the effective reflection coefficient for a plane wave incident from region 2 onto a series of layers.

For the TM, results below a “~” mean that TM parameters (as opposed to TE parameters) are used. Thus,

$$\begin{aligned} r_{\text{TM}} = & \int_{-\infty}^{\infty} ds_2 \tilde{f}^*(s_2) \tilde{f}(s_2) \tilde{R}(s_2) \\ & + \frac{n_2}{n_1} \int_{-\infty}^{\infty} ds_2 (1 + \tilde{R}(s_2)) \left[ \tilde{f}(s_2^*) + \int_{-\infty}^{\infty} ds'_2 \Delta \tilde{D}(s_2, s'_2) \right] \\ & \cdot \left\{ \frac{\tilde{\Delta}^A(s_2)}{2h_1^0(s_2)} + \frac{\tilde{\Delta}^B(s_2)}{2n_1^0} \right\} \\ & + \int_{-\infty}^{\infty} ds_2 (1 + \tilde{R}(s_2) \tilde{f}(s_2)) \int_{-\infty}^{\infty} ds'_2 \Delta D(s_2, s'_2) \tilde{f}^*(s'_2), \quad (10) \end{aligned}$$

where

$$\Delta \tilde{D}(s_2, s'_2) = \frac{n_2}{\lambda_0} \int_{-\infty}^{\infty} dx e^{ik_0 n_2 (s_2 - s'_2)x} \left[ \frac{n_1^0}{n_1(x)} - 1 \right], \quad (11)$$

$$\tilde{\Delta}^{A(0)}(s_2) = \int ds'_2 (1 - \tilde{R}(s'_2)) \tilde{f}(s'_2) \Delta h(s_2, s'_2), \quad (12)$$

$$\tilde{\Delta}^{B(0)}(s_2) = \int ds'_2 (1 + \tilde{R}(s'_2)) \tilde{f}(s'_2) \Delta n(s_2, s'_2), \quad (13)$$

$$\begin{aligned} \tilde{\Delta}^{A(i)}(s_2) = & \tilde{\Delta}^{A(0)}(s_2) + \int_{-\infty}^{\infty} ds'_2 \\ & \cdot \left\{ \tilde{\Delta}^{A(i-1)}(s'_2) \frac{[-(1 + \tilde{R}(s'_2))]}{2h_1^0(s'_2)} + \tilde{\Delta}^{B(i-1)}(s'_2) \frac{[1 - \tilde{R}(s'_2)]}{2n_1^0} \right\} \Delta h(s_2, s'_2), \quad (14) \end{aligned}$$

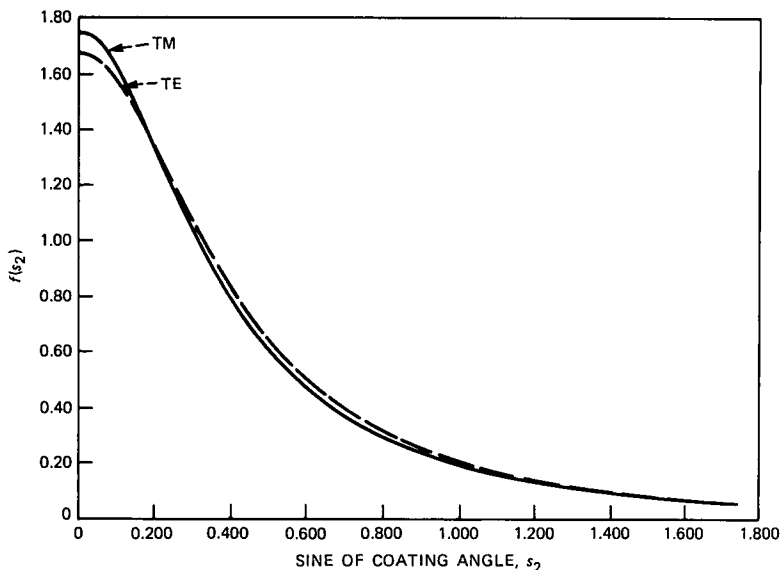


Fig. 2—The  $k$ -space wave functions of TE and TM modes. Solid curve is TE mode and dashed curve is TM mode.

$$\tilde{\Delta}^{B(i)}(s_2) = \tilde{\Delta}^{B(0)}(s_2) + \int_{-\infty}^{\infty} ds'_2 \cdot \left\{ \tilde{\Delta}^{A(i-1)}(s'_2) \frac{[1 + \tilde{R}(s'_2)]}{2h_1^0(s'_2)} - \tilde{\Delta}^{B(i-1)}(s'_2) \frac{[1 - \tilde{R}(s'_2)]}{2n_1^0} \right\} \Delta n(s_2, s'_2), \quad (15)$$

and

$$\Delta h(s_2, s'_2) = \frac{n_2}{\lambda_0} \int_{-\infty}^{\infty} dx e^{ik_0 n_2 (s_2 - s'_2)x} [h_1(s_2, x) - h_1^0(s_2)], \quad (16)$$

and

$$\Delta n(s_2, s'_2) = \frac{n_2}{\lambda_0} \int_{-\infty}^{\infty} dx e^{ik_0 n_2 (s_2 - s'_2)x} [n_1(x) - n_1^0]. \quad (17)$$

### III. NUMERICAL CALCULATIONS

We now calculate several of the terms given in eqs. (1) through (17).

#### 3.1 Determination of $f(s_2)$

The terms,  $f(s_2)$ , are the Fourier transforms of the incident wave function, according to eq. (4). The wave function,  $\psi(x, z)$ , is calculated by solving Maxwell equations in the infinite waveguide defined by  $n_1(x)$ . The wave functions used in the calculations below are the lowest-order TE mode and the lowest-order TM mode. The  $k$ -space wave functions are shown in Fig. 2.

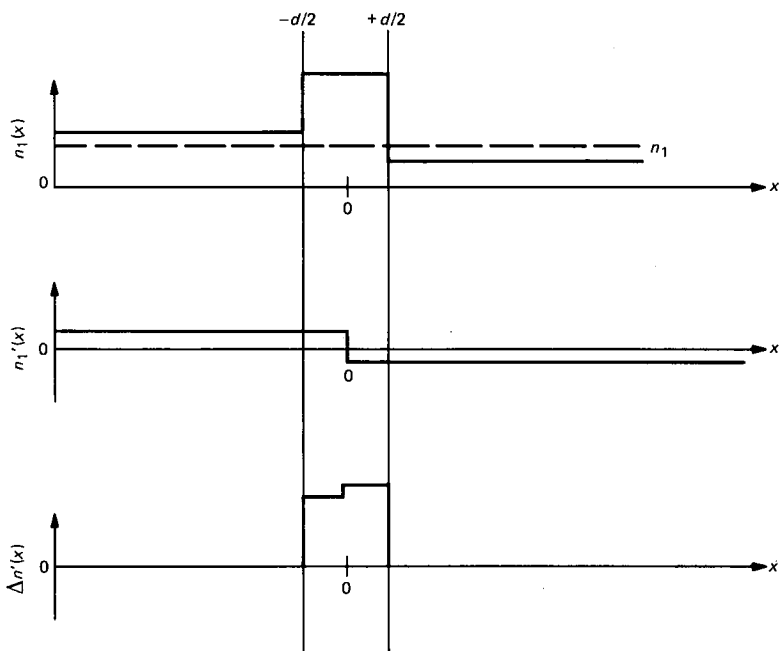


Fig. 3—Details of index step for an asymmetric waveguide.

### 3.2 Determination of $\Delta n(s_2, s_2')$

The correction integral,  $\Delta n(s_2, s_2')$  in eq. (17), determines the strength of the correction term. For a symmetric step waveguide of thickness  $d$ ,  $\Delta n(s_2, s_2') = \frac{\Delta n d n_2}{\lambda_0} \left[ \frac{\sin u}{u} \right]$ , where  $u = \frac{2\pi n_2 d}{\lambda_0} (s_2 - s_2')$ .

For real waveguide devices the index of refraction of the two cladding layers is not, in general, identical. Under these conditions  $\Delta n(x)$  does not approach zero as  $x$  approaches  $\pm\infty$ . We must, therefore, show that the calculation of  $\Delta n(s_2, s_2')$  for an asymmetric waveguide leads to a finite result. As Fig. 3 shows,  $n_1(x)$  is broken into three terms:  $n_1(x) = n_1 + n_1'(x) + \Delta n'(x)$ . From eq. (8) we obtain

$$\begin{aligned} \Delta n(s_2, s_2') &= \frac{n_2}{\lambda_0} \int_{-\infty}^{\infty} dx e^{ik_0 n_2 x (s_2 - s_2')} (n_1'(x) + \Delta n'(x)) \\ &= \frac{n_2}{\lambda_0} \int_{-\infty}^{\infty} dx e^{ik_0 n_2 x (s_2 - s_2')} n_1'(x) + \frac{n_2}{\lambda_0} \int_{-\infty}^{\infty} dx e^{ik_0 n_2 x (s_2 - s_2')} \Delta n'(x). \quad (18) \end{aligned}$$

The problem is solved by placing the system in a large box of length  $2b$  where the length is defined along the  $x$  axis. The box then defines

the allowed values of  $k_x$ . By invoking periodic boundary conditions,  $k_x$  is quantized such that

$$k_x = m\delta k_0, \quad (19)$$

where  $\delta k_0 = (2\pi)/b$  and  $m$  is an integer.

The first integral in expression (18) then becomes

$$\frac{n_2}{\lambda_0} \int_{-b}^b dx e^{i\frac{2\pi}{b}(m-m')x} n_1'(x) \propto [\cos(2\pi(m - m')) - 1] = 0. \quad (20)$$

We next allow  $b$  to approach infinity. Then,  $\Delta n(s_2, s_2')$  is calculable with the modified step defined by  $\Delta n'(x)$ . This is a finite result for any guiding structure. Note that to solve the problem self-consistently,  $\psi$  must be recalculated for an asymmetric waveguide. In a similar manner,  $\Delta h(s_2, s_2')$  [eq. (16)] and  $\Delta H(s_2, s_2')$  [eq. (9)] can be calculated for an asymmetric waveguide.

### 3.3 Calculation of $R(s_2)$ and $\tilde{R}(s_2)$

$R$  and  $\tilde{R}$  are calculated in eq. (5) and are used in eqs. (1) and (10). Since the integrals extend from  $-\infty$  to  $+\infty$ ,  $R(s_2)$  must be calculated for all values of  $s_2$ . There are three critical angles involved, as shown in Fig. 4:

$$\begin{aligned} s_{1c} &= \frac{n_3}{n_2} \\ s_{2c} &= 1 \\ s_{3c} &= \frac{n_1^0}{n_2}. \end{aligned} \quad (21)$$

For  $s_2 < s_{1c}$  an incident wave in region 1 is coupled to a reflected wave in region 1, two plane waves in region 2, and a transmitted plane wave in region 3.

For  $s_{2c} < s_2 < s_{3c}$  an incident wave is coupled to a reflected wave in region 1, plane waves in region 2, and an evanescent field in region 3.

When  $s_{2c} < s_2 < s_{3c}$  a wave incident in region 1 is coupled to evanescent fields in regions 2 and 3 and to a reflected wave in region 1.

When  $s_2 > s_{3c}$  all the fields are evanescent fields.

The real and imaginary parts of  $R(s_2)$  are plotted in Fig. 5a for a normalized coating thickness,  $h = 0$ , where  $h = tn_2/\lambda_0$ . Shown in Fig. 5b are the real and imaginary parts of the product  $R(s_2)|f|^2$ , which correspond to the integrand of the first term in eq. (1). Figures that are similar to Figs. 5a and b but are for the case of  $h = 1/4$  are plotted in Figs. 6a and b. Note that the terms can be both positive and negative

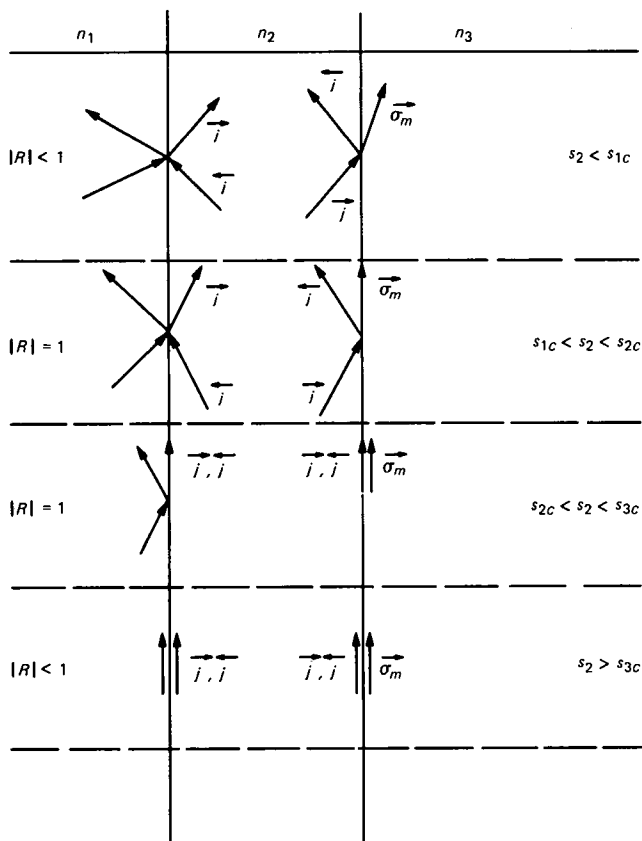


Fig. 4—The  $k$ -vectors for states involved in the calculation of  $R(s_2)$  for all values of  $s_2$ .

and that a minimization may correspond to a balancing of the positive and negative parts of the integral. The cusps in the real and imaginary parts of  $R(s_2)$  occur at the first critical angle. In the region of total reflection (from  $s_2 = s_{2c}$  to  $s_2 = s_{3c}$ )  $|R(s_2)|$  is equal to 1. The phase of the reflection coefficient varies in this region such that the real and imaginary parts of  $R(s_2)$  take values between  $-1$  and  $+1$ .

When the normalized thickness,  $h$ , is  $\sim 0.25$ , the relative weight of large  $s_2$  terms ( $s_2 \geq 0.6$ ) is much more significant. Therefore, any calculation of  $r_{TE}$  or  $r_{TM}$  that is limited to the region of small incident angles is invalid for antireflection coatings.

#### IV. RESULTS

To demonstrate the above formalism, we have performed reflectivity calculations for a  $\lambda_0 = 1.3 \mu\text{m}$  laser with an index of refraction of 3.51

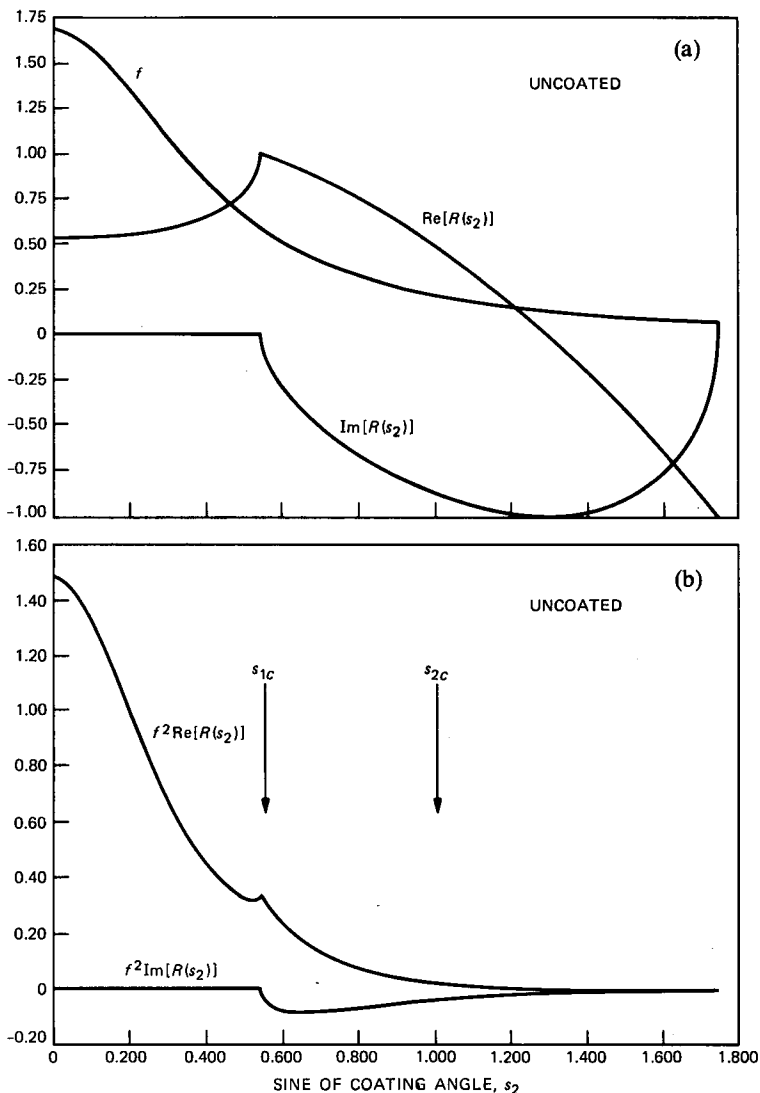


Fig. 5—Real and imaginary parts of (a)  $R(s_2)$  for  $h = 0$ , and (b)  $R(s_2)|f|^2$  for  $h = 0$ .  $f(s_2)$  is shown for comparison.

for the active region and 3.22 for both cladding layers and with an active layer thickness of 0.2 micron. We have limited the calculations to the zeroth-order correction term.

The optimum reflectivity,  $r^{\text{opt}}(n_2)$ , is defined as the minimum of the  $r(h)$  curve for a given coating index  $n_2$ . In Fig. 7  $r^{\text{opt}}(n_2)$  is plotted for various conditions. In all of these calculations the incident wave function is the zeroth mode of the laser waveguide described above.

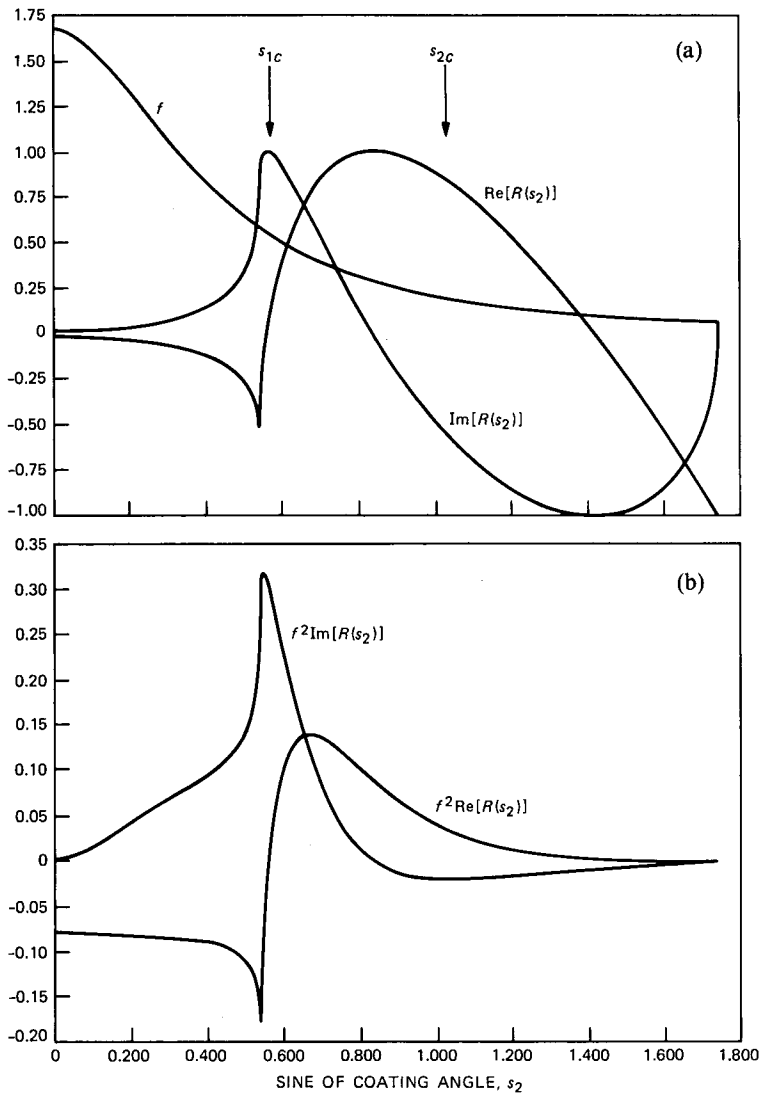


Fig. 6—Real and imaginary parts of (a)  $R(s_2)$  for  $h = 1/4$ , and (b)  $R(s_2)|f|^2$  for  $h = 1/4$ .  $f(s_2)$  is shown for comparison.

The solid curves show the approximation in which the index of refraction of the laser is assumed to be constant and equal to that of the active layer. The dashed curves correspond to our calculations in which the correction terms are neglected. The dotted curves represent the calculation with the zeroth-order correction term included. Note that the result that includes the correction term lies between the results arrived at by assuming the index of the laser is a constant

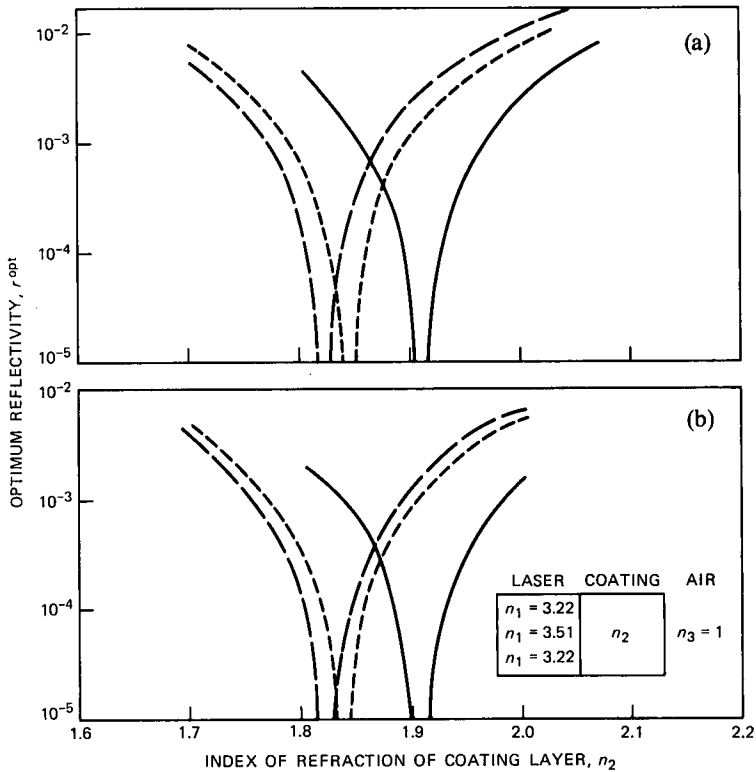


Fig. 7—Optimum reflectivity as a function of index of refraction of coating for (a) TE and (b) TM modes for laser structure shown in inset.

equal to the active area and the result in which the constant index is equal to that of the cladding.

Figure 7 demonstrates the significance of the error obtained when approximating the index of refraction inside the laser as a constant equal to the index of refraction of the active layer. The results shown in Fig. 7 are very similar for both the TE and the TM results. For the TE case the reflectivity is minimized at a coating index of refraction equal to 1.845. For the TM case the minimum occurs at a coating index of refraction equal to 1.840.

Although both the TE and TM reflectivities are minimized by an optimum coating index that is very similar, the coating thicknesses at which this minimum occurs are different. This is shown in Fig. 8, where both the TE and the TM curves are plotted as a function of the coating thickness for a coating index of refraction of 1.840. The thickness for which the reflectivity is minimized is greater for the TE case than for the TM case. When the TE reflectivity is less than  $10^{-5}$ , the TM reflectivity is approximately  $4 \times 10^{-3}$ .

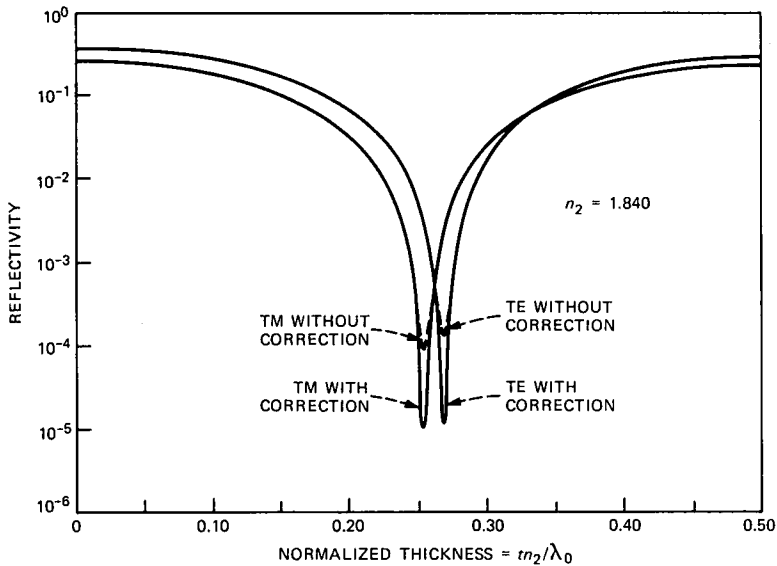


Fig. 8—Reflectivity as a function of normalized thickness for a coating index of 1.840.

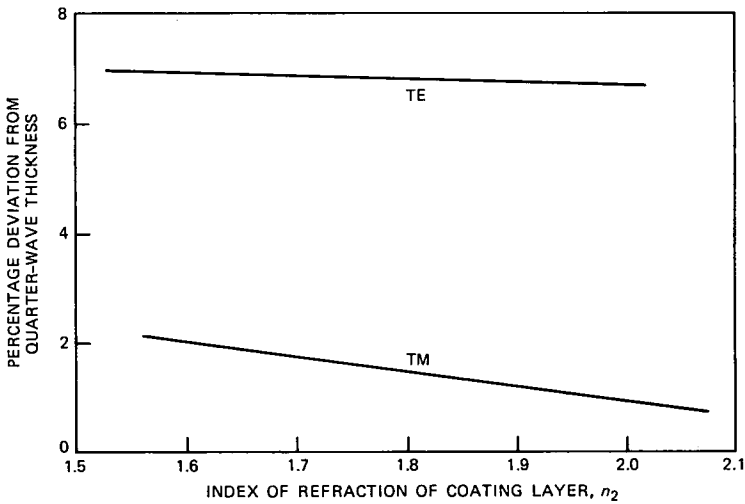


Fig. 9—Percentage deviation from quarter-wave condition of optimum normalized thickness of coating layer as a function of index of refraction of coating layer.

From Fig. 8 we learn that to maintain the reflectivity of the TE component below  $10^{-4}$ , the film thickness must be controlled to within  $\pm 17\text{\AA}$ ; to maintain the reflectivity below  $10^{-3}$  the film thickness must be held to  $\pm 44\text{\AA}$ . The same conditions for the TM component correspond to  $\pm 17\text{\AA}$  and  $\pm 53\text{\AA}$ , respectively.

In Fig. 9 the percentage deviation of the coating (at the minimum

reflectivity) from the quarter-wave thickness is plotted as a function of the index of refraction of the coating for the TE and TM cases. Because the curves never cross, it will not be possible to simultaneously minimize both the reflectivity for the TE and the TM components at a level below  $\approx 10^{-4}$ . The TE deviation is approximately 7 percent over the range considered. The TM deviation varies from 2 percent to 1 percent.

The calculations can be compared with previous modal reflectivity results at  $h = 0$ . In agreement with these calculations,<sup>5</sup> the TE reflectivity is higher than the plane-wave result and the TM reflectivity is lower than the plane-wave result.

## V. CONCLUSIONS

We have derived an exact solution to the coated waveguide reflectivity problem. The solution is valid for an arbitrary index variation,  $n_1(x)$ , of the waveguide structure.

We have observed significant deviations between the exact results and the results obtained when the index of the waveguide structure is approximated as a constant equal to the active layer index.

The range of the indices of refraction and the thickness of the coating layer to minimize either the TE or the TM reflectivity were obtained. The TE and TM reflectivities have their minima at different thicknesses. This suggests that tailoring the output polarization of light-emitting devices by controlling the coating parameters might be possible.

Also, we have outlined the procedure for calculating the parameters to minimize the optical reflectivity. A sample calculation has been given for a particular laser structure. Further work is necessary to set up general guidelines for coating parameters for the various laser structures.

## VI. ACKNOWLEDGMENTS

The authors wish to express their appreciation to W. B. Joyce and to F. K. Reinhart for many helpful discussions and for critical comments on the paper.

## REFERENCES

1. J. McKenna, "The Excitation of Planar Dielectric Waveguides at p-n Junctions, I," *B.S.T.J.*, 46, No. 7 (September 1967), pp. 1491-526.
2. F. K. Reinhart, I. Hayashi, and M. B. Panish, "Mode Reflectivity and Waveguide Properties of Double-Heterostructure Injection Lasers," *J. Appl. Phys.*, 42 (October 1971), pp. 4466-79.
3. E. I. Gordon, "Mode Selection in GaAs Injection Lasers Resulting From Fresnel Reflection," *IEEE J. Quant. Electron.*, QE-9 (July 1973), pp. 772-6.
4. D. C. Krupka, "Selection of Modes Perpendicular to the Junction Plane in GaAs

- Large-Cavity Double-Heterostructure Lasers," *IEEE J. Quant. Electron.*, *QE-11* (July 1975), pp. 390-400.
5. T. Ikegami, "Reflectivity of Mode of Facet and Oscillation Mode in Double-Heterostructure Injection Lasers," *IEEE J. Quant. Electron.*, *QE-8* (June 1972), pp. 470-6.
  6. M. A. A. Pudensi and L. G. Ferreira, "Method to Calculate the Reflection and Transmission of Guided Waves," *J. Opt. Soc. Am.*, *F2* (January 1982), pp. 126-30.
  7. J. E. Kardontchik, "Mode Reflectivity of Narrow Stripe-Geometry Double Heterostructure Lasers," *IEEE J. Quant. Electron.*, *QE-18* (August 1982), pp. 1279-86.
  8. R. H. Clarke, "Theory of Reflection From Antireflection Coatings," *B.S.T.J.*, *62* (December 1984), pp. 2885-92.
  9. L. Lewin, "A Method for the Calculation of the Radiation-Pattern and Mode-Conversion Properties of a Solid-State Heterojunction Laser," *IEEE Trans. Microw. Theory and Tech.*, *MTT-23*, No. 7 (July 1975), pp. 576-85.
  10. M. Born and E. Wolfe, *Principles of Optics*, Fifth Edition, New York: Pergamon, 1975.

## APPENDIX A

### TE Reflectivity

We will use a bra-ket notation,  $(| \ )$ , in the following derivation for simplicity of notation. In this context a bra-ket denotes integration over the  $x$  coordinate only. Therefore, the bra-ket depends on the  $z$  coordinate. Some of the bra-kets involve integrations over products of functions defined in adjacent regions. These integrals only have meaning when evaluated at the boundary between these regions. Equation (22) is a summary of some basis states used in the calculation and some elementary integrals needed later. To further simplify the notation, the system is placed in a large box of unit volume. The integrals in the main text of the paper are derived from the sums presented in this section by allowing the volume to approach infinity. Note that in this section the continuous variable  $s_2$  has been replaced by the discrete variable  $j$ .

The incident wave function in region 1 is

$$|\vec{j}\rangle = e^{ik_1z} g(x) \quad (22a)$$

$$|\vec{j}\rangle = e^{-ik_1z} g(x). \quad (22b)$$

Basis states in region 2 are

$$|\vec{j}\rangle = \frac{1}{\sqrt{\lambda_2}} e^{ik_z^j z} e^{ik_x^j x}, (k_z^2 + k_x^2 = k_2^2 = (k_0 n_2)^2), (k_z^j = k_z^{-j}) \quad (22c)$$

$$|\vec{j}\rangle = \frac{1}{\sqrt{\lambda_2}} e^{ik_z^j z} e^{ik_x^j x} \quad (22d)$$

$$(\vec{j}|\vec{j}') = e^{-2ik_z^j z} \delta_{jj'} \quad (22e)$$

$$(\vec{j}|\vec{j})|_{z=0} = f_j \quad (22f)$$

$$(\bar{j}|\bar{\psi})|_{z=0} = (\bar{j}|\bar{\psi})|_{z=0} = (\bar{j}|\bar{\psi})|_{z=0} = f_j \quad (22g)$$

$$(\bar{\psi}|\bar{\psi})|_{z=0} = \sum_j f_j f_j^* \quad (22h)$$

In the above expressions  $g(x)$  corresponds to the real space modal distribution and  $\delta_{jj'}$  is a Kronecker delta function.

There is a one-to-one correspondence between the wave functions  $\bar{j}$ ,  $\bar{j}$  and the wave function  $\bar{\sigma}_m$ , where the wave function  $\bar{j}$  corresponds to a state in region 2 and  $\bar{\sigma}_m$  corresponds to a state in region 3. This correspondence is due to the uniformity of the interface between regions 2 and 3. Thus we may write

$$(\bar{j}|\bar{\sigma}_m)|_{z=t} = \delta_{mj} \alpha_m, \quad (23)$$

where  $\alpha_m$  is a constant.

The following calculation consists of demanding continuity of the tangential components of the electric and magnetic fields at the two interfaces. The wave functions,  $\bar{\psi}$ , represent the electric fields. The magnetic fields may be easily obtained by using Maxwell equations. We define an operator,  $h_i$ , which multiplies the plane-wave functions in region  $i$  by the cosine of the angle between the incident  $k$ -vector and the surface normal vector. For the TE fields, in which the electric field is along the  $y$  axis, the magnetic fields can be obtained with operator  $h_i$ :

$$\bar{B}_{\tan \text{TE}}^i \propto n_i(x) h_i |\bar{j}^i\rangle = \mp h_i^j(x) n_i(x) |\bar{j}^j\rangle \quad (24)$$

With the help of Snell's law,<sup>10</sup> we write for the operators

$$\begin{aligned} h_1 &= \sqrt{1 - \left(\frac{n_2 s_2}{n_1}\right)^2}, & s_2 &= \sin \Theta_2 \quad \text{for } |s_2| < 1 \\ h_2 &= \sqrt{1 - s_2^2} \\ h_3 &= \sqrt{1 - \left(\frac{n_2 s_2}{n_3}\right)^2}. \end{aligned} \quad (25)$$

At the surface between regions 2 and 3 the equation describing the continuity of the electric field is written

$$\sum_j [b_j |\bar{j}\rangle + d_j |\bar{j}\rangle] = \sum_m c_m |\bar{\sigma}_m\rangle. \quad (26)$$

The transverse magnetic field continuity equation is written

$$\sum_j [b_j n_2 h_2^j |\bar{j}\rangle - d_j n_2 h_2^j |\bar{j}\rangle] = \sum_m n_3 h_3^m c_m |\bar{\sigma}_m\rangle. \quad (27)$$

Project with  $|\bar{j}\rangle$  on eqs. (26) and (27) and use eqs. (22) and (23) for substitutions to obtain

$$b_j + d_j e^{-2i\phi_j} = c_j \alpha_j \quad (28)$$

$$n_2 h_2^j [b_j - d_j e^{-2i\phi_j}] = n_3 h_3^j c_j \alpha_j, \quad (29)$$

where

$$\phi_j = \frac{2\pi n_2 h_2^j t}{\lambda_0}$$

and where  $\lambda_0$  is the wavelength in vacuum and  $t$  is the thickness of the coating.

Equations (28) and (29) are combined to eliminate  $c_j \alpha_j$ ,

$$d_j = b_j \frac{(n_2 h_2^j - n_3 h_3^j)}{(n_2 h_2^j + n_3 h_3^j)} e^{2i\phi_j} = b_j r_{23}^j e^{2i\phi_j}. \quad (30)$$

The equation for the continuity of the electric field on the surface of regions 1 and 2 is written

$$|\vec{\psi}\rangle + r|\tilde{\psi}\rangle + \sum_k a_k |\vec{\phi}_k\rangle = \sum_j [(b_j|\bar{j}\rangle + d_j|\bar{j}\rangle)]. \quad (31)$$

With the use of the identity operators  $1 = \sum_j |\bar{j}\rangle\langle\bar{j}|$  and  $1 = \sum_j |\bar{j}\rangle\langle\bar{j}|$ , eq. (31) becomes

$$\begin{aligned} \sum_{j'} \left[ f_{j'} |\bar{j}'\rangle + r f_{j'} |\bar{j}'\rangle + \sum_k a_k (\bar{j}' | \vec{\phi}_k) |\bar{j}'\rangle \right] \\ = \sum_{j'} [b_{j'} |\bar{j}'\rangle + d_{j'} |\bar{j}'\rangle]. \quad (32) \end{aligned}$$

With the help of eq. (24), the magnetic field continuity equation is written

$$\begin{aligned} \sum_{j'} \left[ h_1^{j'}(x) n_1(x) [f_{j'} |\bar{j}'\rangle - r f_{j'} |\bar{j}'\rangle] - \sum_k a_k (\bar{j}' | \vec{\phi}_k) h_1^{j'}(x) n_1(x) |\bar{j}'\rangle \right] \\ = \sum_{j'} n_2 h_2^{j'} [b_{j'} |\bar{j}'\rangle - d_{j'} |\bar{j}'\rangle]. \quad (33) \end{aligned}$$

We project on eqs. (32) and (33) with  $|\bar{j}\rangle$  at the surface of regions 1 and 2 ( $z = 0$ ). We must consider that since both  $h_1^{j'}(x)$  and  $n_1(x)$  depend on  $x$ ,  $(\bar{j} | h_1^{j'}(x) n_1(x) | \bar{j}') \neq h_1^{j'}(x) n_1(x) (\bar{j} | \bar{j}')$ .

We obtain

$$f_j + f_j r + \sum_k a_k (\bar{j} | \vec{\phi}_k) = b_j + d_j \quad (34)$$

$$\sum_{j'} \left( f_{j'} - f_j r - \sum_k a_k(\tilde{\gamma}' | \tilde{\phi}_k) \right) (\tilde{\gamma} | h_1^{j'}(x) n_1(x) | \tilde{\gamma}') = n_2 h_2^j (b_j - d_j). \quad (35)$$

We now rewrite the product  $n_1(x)h_1^j(x)$  as discussed in the main text,

$$n_1(x)h_1^j(x) = n_1^0 h_1^0 + \Delta H_j, \quad (36)$$

where

$$h_1^0 = \sqrt{1 - \left( \frac{n_2 s_2}{n_1^0} \right)^2}$$

and combine eqs. (34) and (35) to obtain

$$f_j [r_{12}^j + 1] + \frac{\Delta_j}{(n_1 h_1^j + n_2 h_2^j)} = b_j [1 + r_{12}^j r_{23}^j e^{2i\phi_j}], \quad (37)$$

where  $r_{12}^j$  and  $r_{23}^j$  are the plane boundary Fresnel reflection coefficients and

$$\Delta_j = \sum_{j'} \left[ f_{j'} - f_j r - \sum_k a_k(\tilde{\gamma}' | \tilde{\phi}_k) \right] (\tilde{\gamma} | \Delta H_{j'} | \tilde{\gamma}') |_{z=0}. \quad (38)$$

To calculate  $r$  we project  $|\tilde{\psi}_j$  on eq. (31) at  $z = 0$  and use the fact that  $|\tilde{\psi}_j$  is orthogonal to  $|\tilde{\phi}_k$  to obtain

$$r = \sum_j f_j^* (b_j + d_j - f_j). \quad (39)$$

If we use eq. (30) to substitute for  $d_j$ , eq. (37) to substitute for  $b_j$ , and eq. (5) to define  $R_j$  we obtain eq. (1), the desired result. The last step in the calculation requires that the box dimensions approach infinity so that the sum tends to an integral.

The expansion for  $\Delta_j$  is obtained by equating like terms in eqs. (1) and (39), and using eq. (34) to replace  $b_j + d_j - f_j$ . We obtain

$$f_j r + \sum_k a_k(\tilde{\gamma} | \tilde{\phi}_k) = f_j R_j + \Delta_j \frac{[R_j + 1]}{2n_1^0 h_1^0}. \quad (40)$$

If (40) is substituted into (38), we obtain eqs. (2) and (3).

## APPENDIX B

### TM Reflectivity

The TM field is analyzed in close analogy to the TE field. In this case the magnetic field is along the  $y$  axis. The operator,  $h_i$ , is useful

to determine, for a given angle  $\Theta$ , the tangential component of the electric field vector. To obtain the magnetic field, the wave function is multiplied by the index of refraction. With these considerations the two equations representing continuity at the surface of regions 2 and 3, after projecting on  $|\tilde{j}\rangle$ , are written

$$n_2(\tilde{b}_j + \tilde{d}_j e^{-2i\phi_j}) = n_3 \tilde{c}_j \tilde{\alpha}_j \quad (41)$$

$$h_2^j(\tilde{b}_j - \tilde{d}_j e^{-2i\phi_j}) = h_3^j \tilde{c}_j \tilde{\alpha}_j. \quad (42)$$

Combining eqs. (41) and (42) to eliminate  $\tilde{\alpha}_j \tilde{c}_j$ , we obtain

$$\tilde{d}_j = \tilde{b}_j \frac{(n_3 h_2^j - n_2 h_3^j)}{(n_3 h_2^j + n_2 h_3^j)} e^{2i\phi_j} = \tilde{b}_j \tilde{r}_{23} e^{2i\phi_j}. \quad (43)$$

The conditions for continuity of the electric field and magnetic field at the surface between regions 1 and 2 are written

$$h_1 |\tilde{\psi}\rangle + h_1 r |\tilde{\psi}\rangle + \sum_k h_1 \tilde{a}_k |\tilde{\phi}_k\rangle = h_2 \left[ \sum_j \tilde{b}_j |\tilde{j}\rangle + \tilde{d}_j |\tilde{j}\rangle \right] \quad (44)$$

$$n_1(x) \left[ |\tilde{\psi}\rangle + r |\tilde{\psi}\rangle + \sum_k \tilde{a}_k |\tilde{\phi}_k\rangle \right] = n_2 \left[ \sum_j (\tilde{b}_j |\tilde{j}\rangle + \tilde{d}_j |\tilde{j}\rangle) \right]. \quad (45)$$

After using the identity operator, projecting on  $|\tilde{j}\rangle$ , and using the fact that at  $z = 0$   $(\tilde{j} | n_1(x) | \tilde{j}') = (\tilde{j} | n_1(x) | \tilde{j}')$  and  $(\tilde{j} | h_1^j(x) | \tilde{j}') = -(\tilde{j} | h_1^j(x) | \tilde{j}')$  [see eq. (24)], we get

$$h_1^0 \tilde{f}_j - \tilde{r} h_1^0 \tilde{f}_j - h_1^0 \sum_k \tilde{a}_k (\tilde{j} | \tilde{\phi}_k) + \tilde{\Delta}_j^A = h_2^j (\tilde{b}_j - \tilde{d}_j) \quad (46)$$

and

$$n_1^0 \tilde{f}_j - n_1^0 \tilde{r} \tilde{f}_j + n_1^0 \sum_k \tilde{a}_k (\tilde{j} | \tilde{\phi}_k) + \tilde{\Delta}_j^B = n_2 (\tilde{b}_j + \tilde{d}_j), \quad (47)$$

where

$$\tilde{\Delta}_j^A = \sum_{j'} (\tilde{f}_{j'} - \tilde{r} \tilde{f}_{j'} - \sum_k \tilde{a}_k (\tilde{j}' | \tilde{\phi}_k)) (\tilde{j} | h_1^j(x) - h_1^0 | \tilde{j}') \quad (48)$$

and

$$\tilde{\Delta}_j^B = \sum_{j'} (\tilde{f}_{j'} + \tilde{r} \tilde{f}_{j'} + \sum_k \tilde{a}_k (\tilde{j}' | \Delta n(x) | \tilde{j}')). \quad (49)$$

Combine eqs. (46) and (47) by multiplying (46) by  $n_1^0$  and (47) by  $h_1^0$  and then adding them together. Use the fact that

$$\tilde{r}_{12} = \frac{n_2 h_1 - n_1 h_2}{n_2 h_1 + n_1 h_2}$$

to get

$$\tilde{b}_j = \frac{\frac{n_1^0}{2n_2} [1 + \tilde{r}_{12}^j] \left[ 2\tilde{f}_j + \frac{\tilde{\Delta}_j^A}{h_1^0} + \frac{\tilde{\Delta}_j^B}{n_1^0} \right]}{[1 + \tilde{r}_{12}^j \tilde{r}_{23}^j e^{2i\phi_j}]} \quad (50)$$

The reflection coefficient is then derived by dividing eq. (45) by  $n_1(x)$  and then projecting on  $|\tilde{\psi}\rangle$ , so that

$$\langle \tilde{\psi} | \tilde{\psi} \rangle + \tilde{r} = n_2 \sum_j \left( \tilde{\psi} \left| \frac{1}{n_1(x)} \right| \tilde{j} \right) (\tilde{b}_j + \tilde{d}_j). \quad (51)$$

Expand  $1/n_1(x)$  as

$$\frac{1}{n_1(x)} = \frac{1}{n_1^0} + \frac{1}{n_1^0} \left[ \frac{n_1^0}{n_1(x)} - 1 \right] \quad (52a)$$

$$= \frac{1}{n_1^0} [1 + \Delta D(x)]. \quad (52b)$$

We then define

$$\Delta \tilde{D}_{jj'} = \left( \tilde{j}' \left| \frac{n_1^0}{n_1(x)} - 1 \right| \tilde{j} \right) \quad (52c)$$

and combine eqs. (51) with (52) to obtain

$$\sum_j \tilde{f}_j^* \tilde{f}_j + \tilde{r} = \frac{n_2}{n_1^0} \sum_j \left[ \tilde{f}_j^* + \sum_{j'} \Delta \tilde{D}_{jj'} \tilde{f}_{j'}^* \right] \tilde{b}_j (1 + \tilde{r}_{23} e^{2i\phi_j}). \quad (53)$$

Now substitute (50) for  $b_j$  to yield an expression for the reflection coefficient:

$$\begin{aligned} \tilde{r} = \sum_j \tilde{f}_j^* \tilde{f}_j \tilde{R}_j + \sum_j \tilde{f}_j^* [1 + \tilde{R}_j] \left[ \tilde{f}_j^* + \sum_{j'} \Delta \tilde{D}_{jj'} \tilde{f}_{j'}^* \right] \left[ \frac{\tilde{\Delta}_j^A}{2h_1^0} + \frac{\tilde{\Delta}_j^B}{2n_1^0} \right] \\ + \sum_j \left[ \sum_{j'} \Delta \tilde{D}_{jj'} \tilde{f}_{j'}^* \right] [1 + \tilde{R}_j] \tilde{f}_j. \end{aligned} \quad (54)$$

We must now form a series expansion for  $\tilde{\Delta}_j^A$  and  $\tilde{\Delta}_j^B$ .

Combining eqs. (47) and (43) and (50) we get

$$\tilde{r} \tilde{f}_j + \sum_k \tilde{a}_k (\tilde{j} | \tilde{\phi}_k) = \tilde{R}_j \tilde{f}_j + [1 + \tilde{R}_j] \frac{\tilde{\Delta}_j^A}{2h_1^0} - [1 - \tilde{R}_j] \frac{\tilde{\Delta}_j^B}{2n_1^0}. \quad (55)$$

Equation (55) is now plugged into (48) and (49) to obtain eqs. (12) through (15).

## AUTHORS

**Peter P. Deimel**, Dipl. Phys. (Physics), 1974, Technical University in Munich; Ph.D. (Physics), 1980, University of Oregon; AT&T Bell Laboratories, 1980—. Mr. Deimel's initial work involved coupling semiconductor lasers to a grating and wavelength tuning. His recent work involves integral lens calculations, and he is currently working on problems in monolithic integrated optoelectronics.

**Daniel R. Kaplan**, B.S. (Physics), 1977, State University of New York at Albany; M.A. (Physics), 1979, Ph.D. (Physics), 1981, Princeton University; Institute for the Study of Defects in Solids (I.S.D.S.), Albany, 1976; Brookhaven National Laboratories, Physics Department, Summer 1978 and Summer 1979; AT&T Bell Laboratories, 1979—. At I.S.D.S. Mr. Kaplan worked on Extended Huckel Theory Calculations of impurities in silicon and on RBS measurements of impurity diffusion in silicon. At Brookhaven Labs he worked on RBS analysis and nuclear reaction analysis of the diffusion of oxygen in alumina. His doctoral work, performed while at AT&T Bell Laboratories from 1979 to 1981, consisted of measurements of inelastic scattering from X-ray standing waves. Since 1981 he has been involved in lightwave communications, and his current work is in monolithic integrated optoelectronics.